Journal of Electroceramics 3:4, 399–407, 1999

Structure and Electrical Properties of Ni-substituted Lanthanum Gallate Perovskites

N.J. LONG & F.' LECARPENTIER
[1]*Industrial Research Limited, Gracefield Rd, PO Box 31-310, Lower Hutt, New Zealand*

H.L. TULLER
Crystal Physics and Electroceramics Laboratory, Department of Materials Science and Engineering, Massachusetts Institute of Technology, Cambridge, MA 02139, U.S.A.

Submitted February 19, 1999; Revised April 16, 1999; Accepted April 16, 1999

Abstract. Crystal structure, electrical conductivity and thermal expansion of materials in the system $La_{0.9}Sr_{0.1}Ga_{1-y}Ni_yO_3$ (LSGN) with $0 < y \leq 0.5$ have been studied as a function of Ni content, temperature and P_{O_2}. The materials have an orthorhombic structure at low dopant content and a hexagonal structure for higher Ni content. The $\sigma(P_{O_2}, T)$ results show increasing electronic conductivity at high P_{O_2} with increasing Ni content. At low P_{O_2} the conductivity fits a model for predominant ionic conductivity. AC impedance spectroscopy on an electron blocking cell of the form M/LSG/LSGN/LSG/M was used to isolate the ionic conductivity in the $y = 0.1$ and 0.2 materials. The materials were found to have appreciable ionic conductivity in air with a similar magnitude and activation energy to the electrolyte materials. An analysis of the low frequency impedance of the blocking cell provided values for $\tilde{D}$ at 800°C of the order of 9×10^{-5} cm^2/s. An evaluation of the so called chemical capacitance enabled determination of the electron density and mobility. The calculated electronic mobility of 3.8×10^{-3} cm^2/Vs and activation energy of 0.14 eV for the $y = 0.2$ material are in excellent agreement with expectations of an electronic transport model involving electron hopping within the Ni impurity band. The thermal expansion coefficients of the Ni doped materials were determined as a function of temperature and dopant level. The presence of mixed conductivity suggests that this material may be useful as an electrode for a lanthanum gallate based fuel cell or other electrochemical device.

Keywords: lanthanum gallate, mixed conductor, fuel cell cathode, blocking cell

1. Introduction

The search for a lower operating temperature solid oxide fuel cell has received a considerable impetus in the last few years with the discovery of the (La,Sr)(Ga,Mg)O_3 (LSGM) electrolyte [1,2]. This material may be an alternative to YSZ as an electrolyte in a commercially viable system which could operate at around 800°C. Electrode materials that would be compatible with LSGM have so far not received much attention. Huang et al. [3,4] have shown that (La,Sr)CoO_3 may be a suitable cathode material but the reactivity of this material with the electrolyte, and thermal expansion compatibility is questionable. In a preliminary report [5], we showed that it is possible to synthesize Ni-doped lathanum gallate (LSGN) materials with significant electronic and ionic conductivity. In this study, we provide a detailed analysis of (1) the dependence of the ionic and electronic conductivity on temperature, P_{O_2} and Ni concentration and (2) the low frequency impedance of an electron blocking cell leading to the derivation of the chemical diffusivity and capacitance and the individual carrier mobilities. In a subsequent article [6], we report on the performance and compatibility of LSGN cathodes with the LSGM

solid electrolyte and discuss its ultimate incorporation into a LSGM-based fuel cell.

For catalytic purposes, a mixed ionic and electronic conducting (MIEC) electrode is preferred over a pure electronic conductor, due to the expansion of the triple phase boundary for oxygen reduction to the whole surface of the mixed conductor. A promising approach to develop a MIEC is to dope the electrolyte material with multivalent cations in order to introduce electronic conductivity [7]. The LSGM oxygen ion conductor is an ideal candidate for this approach given the flexibility to substitute ions on either the A or B sites to enhance the ionic or electronic conductivity. Indeed Ishihara et al. [8] recently reported MIEC in the related gallate $Nd_{0.9}Ca_{0.1}Ga_{0.9}Co_{0.1}O_3$ but with total conductivity limited to ~ 1 S/cm at 1223 K.

In this study the effect of Ni as a B site dopant in $La_{1-x}Sr_xGaO_3$ is investigated. The Sr^{2+} on the La^{3+} sites is compensated by oxygen vacancies giving rise to ionic conductivity [1,2]. The Ni substituted for Ga^{3+} may be in either of the two oxidation states, Ni^{+2} or Ni^{+3}. The ionic radii of Ni^{2+} and Ni^{3+} fall slightly above and below that of Ga^{3+} respectively which should allow Ni in either state to successfully substitute into the compound. We expect that Ni^{2+} may be compensated either by further oxygen vacancies or by holes. $LaNiO_3$ with Ni in the $+3$ oxidation state is known to be a metallic conductor with a relatively narrow conduction band made up of 3d metal orbitals with an admixture of oxygen 2p [9]. We expect, as we add Ni in LSGN to get a hopping conductivity among the Ni sites and eventually a metallic conductivity as we form a Ni or Ni-O hybrid band of sufficient width.

We have measured the temperature and P_{O_2} dependence of the conductivity and will correlate this with a defect model to identify regions of predominant ionic and electronic conductivity. To further characterize the mixed conducting properties of our material, we used an ac impedance technique with electron blocking electrodes. We have previously used this method to measure the ionic transference number in Mn doped gadolinium titanate [10]. This method is particularly useful when $\sigma_e \geq \sigma_i$. The thermal expansion of our materials was measured to investigate their mechanical compatibility with the LSGM electrolyte.

2. Experiment and Theory

Samples of LSGN ($y = 0.05$, 0.10, 0.20 and 0.50) were prepared from starting materials of high purity (99.99%) oxide powders of La_2O_3, $SrCO_3$, Ga_2O_3, and NiO. The powders were mixed in an agate mortar, then pelletized and fired 3 times at 1300°C for 16 h with intermediate regrinding. The final pellets were isopressed at 350 MPa and fired at 1500°C for 48 h. The formation of impurity phases of $SrLaGaO_4$ and $SrLaGa_3O_7$ was avoided if this preparation was followed. The XRD patterns of the samples were obtained using a Philips automated diffractometer and the lattice parameters were determined with the assistance of a computer program.

The total conductivity was obtained from four probe measurements on samples of approximate dimensions $2 \times 2 \times 8$ mm. The different partial pressures of oxygen were obtained by mixing oxygen and nitrogen, or CO and CO_2, in appropriate proportions. The oxygen partial pressure was checked with a zirconia sensor. For the ac measurements components of the blocking cell:

$$O_2,\ M/La_{0.9}Sr_{0.1}GaO_3/La_{0.9}Sr_{0.1}Ga_{0.8}Ni_{0.2}O_3/La_{0.9}Sr_{0.1}GaO_3/M,\ O_2$$

where M = Ag or Pt, were prepared by lightly copressing the pre-reacted powders, isopressing at 350 MPa, and then sintering in air at 1500°C for 48 h. The samples were approximately 7 mm in diameter and 10 mm in length with each component of equal length. SEM analysis showed the samples to be of high density which is important to prevent any leakage of molecular oxygen through the sample. A Solartron low frequency 1260 or 1250 impedance analyzer was used to measure the impedance spectrum and fitting was done using the program ZPlot (Scribner Associates, Inc.). Thermal expansion measurements were carried out on a standard dilatometry rig.

To extract the ionic conductivity from our impedance measurements we followed the analysis of Lee and Yoo [11], based on the circuit model of Maier [12]. The blocking experiment was first analyzed in the time domain by Yokota [13] and more general solutions in the frequency domain have been examined by Franceschetti et al. [14]. At low frequencies, the spectrum contains a Warburg diffusion impedance due to O^{2-} diffusion in the MIEC. The Warburg impedance is fitted to the equation

$$Z_w = R_w \frac{\tanh[\sqrt{i3S\omega}]}{\sqrt{i3S\omega}} \tag{1}$$

This is the solution to a finite length Warburg impedance, where for a double blocking cell,[1] $S = L^2/(12\tilde{D})$, L is the diffusion length (i.e., the thickness of the MIEC), and $\tilde{D}$ is the chemical diffusion coefficient of the MIEC. Z_w reflects the diffusion of oxygen ions in the MIEC at low frequencies. Physically the SE blocks the electrons and the oxygen ions are now driven, in part, by a concentration gradient across the MIEC. From the circuit model given by Lee and Yoo (11) we also have

$$R_W = t_e R_i \tag{2}$$

where R_w is the Warburg resistance, R_i is the ionic resistance of the MIEC and t_e is the electronic transference number. By combining the low frequency fitting with the measured total conductance,

$$1/R_t = 1/R_i + 1/R_e \tag{3}$$

where R_e is the electronic resistance of the MIEC, we are able to separate the ionic conductivity from the total conductivity [10]. For the blocking technique to be valid we must have $R_e^{\mathrm{SE}} \gg R_e^{\mathrm{MIEC}}$ and $R_i^{\mathrm{SE}} \ll R_i^{\mathrm{MIEC}}$ [15]. This ensures that the SE is blocking the electronic current in the mixed conductor, rather than the mixed conductor blocking the ionic current in the SE. There is some uncertainty in the literature as to whether the blocking electrode we have chosen, $La_{0.9}Sr_{0.1}GaO_3$, has appreciable electronic conductivity at high P_{O_2} [16]. Recent results suggest that it has not [17,18]. Our own experiments with Pt blocking electrodes suggest that the electronic conductivity in air must be small [19]. We are therefore confident that the above criterion is satisfied. The use of a lanthanum gallate compound as the blocking SE allows us to co-sinter the MIEC and SE powders. This means leaks or contact resistances at the SE/MIEC boundary are minimized, problems often associated with the use of YSZ as the blocking SE in electrochemical cells.

3. Results and Discussion

The undoped compound $LaGaO_3$ has the orthorhombic structure (JCPDS 24–1102). For small additions of Sr^{2+} for La^{3+} and $Ni^{2+/3+}$ for Ga^{3+} the cell structure is unchanged. At larger concentrations of $Ni^{2+/3+}$, the compound assumes the more symmetrical hexagonal structure. The results of the XRD analysis are shown in Table 1.

The conductivities as a function of temperature, measured in 0.21 atm, for the compounds $La_{0.9}Sr_{0.1}Ga_{1-y}Ni_yO_{3-\delta}$ are shown in Fig. 1. The activation energy is seen to decrease with dopant level and we have a transition from a semiconductor-like conductivity for low dopant concentrations to a metallic conductivity for the highest $Ni^{2+/3+}$ concentration. As $LaNiO_3$ is a metallic conductor with overlapping Ni^{3+} and O^{2-} bands giving the metallic behavior, we interpret our results as the Ni-doped material likewise forming a conduction band of overlapping Ni-3d and O-2p orbitals.

For a more complete analysis of the defect chemistry of these materials we measured the conductivity as a function of P_{O_2}. The $\sigma(P_{O_2}, T)$ results are shown in Figs. 2(a–d). All the materials were stable at low $P_{O_2}(\log P_{O_2} < -8)$ with the exception of LSGN($y = 0.5$). XRD analysis of a

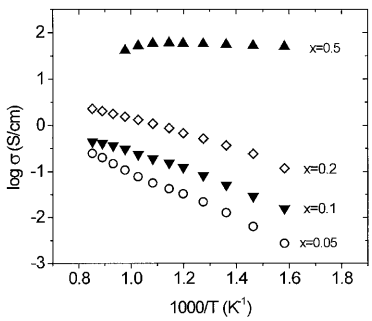

Fig. 1. Temperature dependence of the conductivity for $La_{0.9}Sr_{0.1}Ga_{1-x}Ni_xO_3$, measured in 0.21 atm.

Table 1. Structure parameters of Ni-doped $LaGaO_3$

Compound	Structure	a	b	c
$La_{0.9}Sr_{0.1}GaO_3$	Orthorhombic	5.4897	5.5266	7.7709
$La_{0.9}Sr_{0.1}Ga_{0.95}Ni_{0.05}O_3$	Orthorhombic	5.489	5.531	7.778
$La_{0.9}Sr_{0.1}Ga_{0.9}Ni_{0.1}O_3$	Hexagonal	5.5044		6.6603
$La_{0.9}Sr_{0.1}Ga_{0.8}Ni_{0.2}O_3$	Hexagonal	5.5089		6.6578
$La_{0.9}Sr_{0.1}Ga_{0.5}Ni_{0.5}O_3$	Hexagonal	5.497		6.634

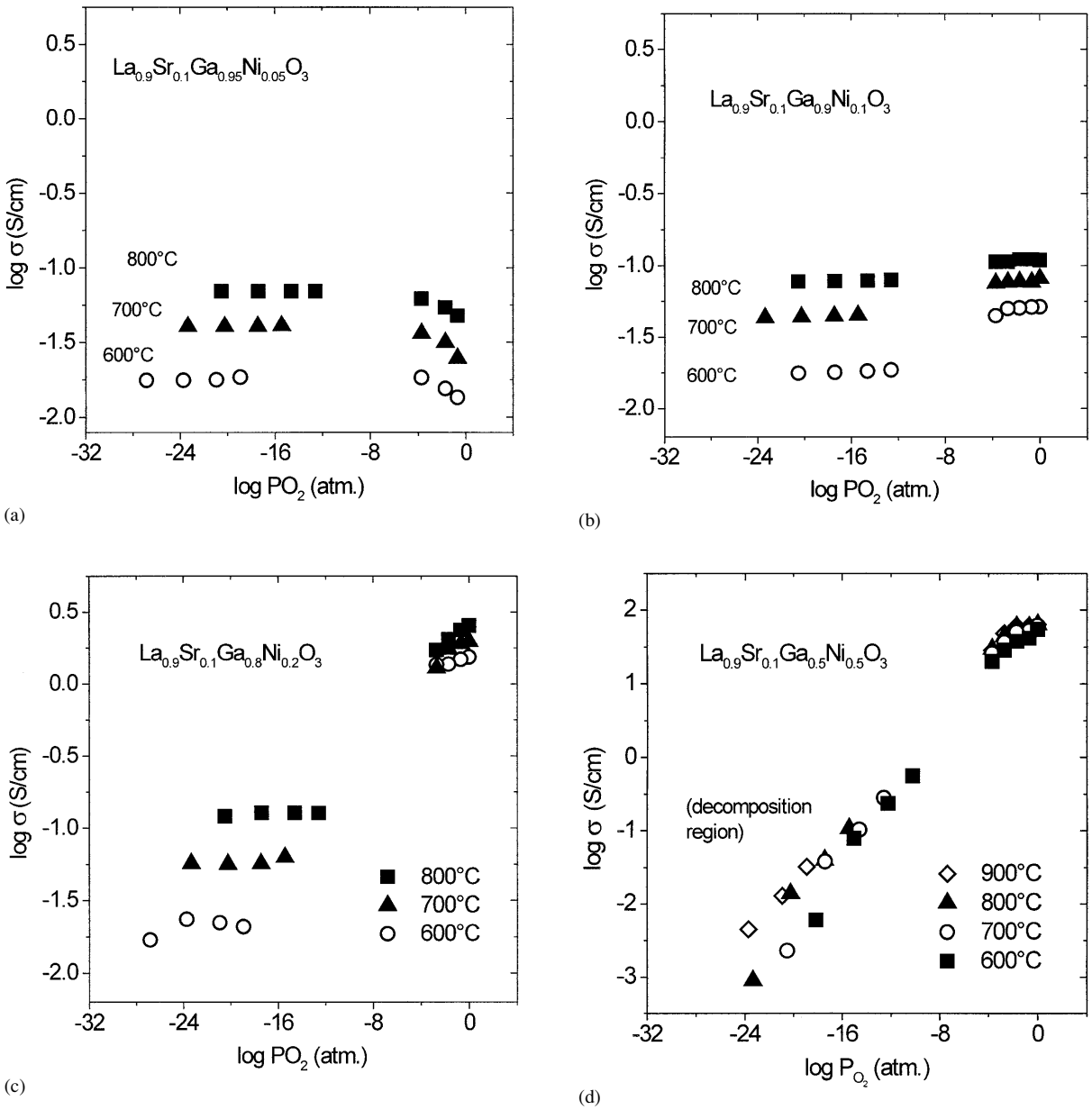

Fig. 2. $\sigma(P_{O_2}, T)$ results for $La_{0.9}Sr_{0.1}Ga_{1-x}Ni_xO_3$ with (a) $x = 0.05$, (b) $x = 0.10$, (c) $x = 0.20$ and (d) $x = 0.50$.

LSGN($y = 0.5$) sample quenched at low P_{O_2} showed decomposition into a mixture of phases.

The P_{O_2} independence of the conductivity at low P_{O_2} suggests the conduction for LSGN ($y = 0.05$, 0.1 and 0.2) is purely ionic in this regime. If we assume that the Ni is in the $2+$ oxidation state and is charge compensated by oxygen vacancies, then at low P_{O_2} we have (using the conventional notation [20]):

$$[Sr_{La}{}'] + [Ni_{Ga}{}'] = 2[V_o^{\cdot\cdot}] \tag{4}$$

Then the ionic conductivity given by:

$$\sigma_i = 2[V_o^{\cdot\cdot}]q\mu_{V_o^{\cdot\cdot}}, \tag{5}$$

should scale with the total dopant concentration. In Fig. 3 we have plotted the conductivity at 800°C versus a normalized dopant concentration. As

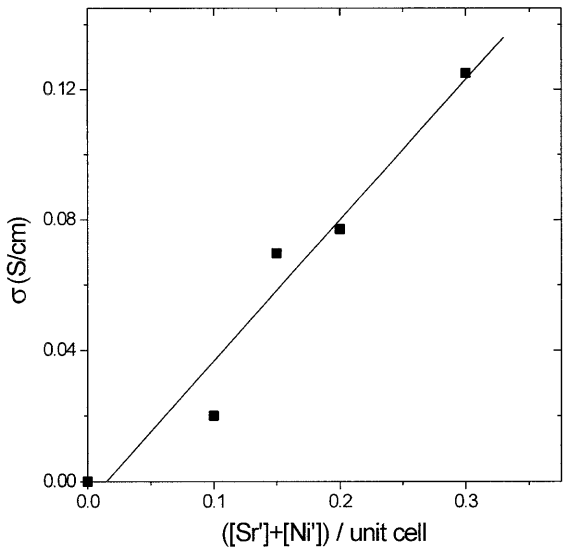

Fig. 3. The ionic conductivity at low P_{O_2} and 800°C as a function of the normalized total dopant content.

expected, this gives approximately a straight line with an intercept through zero. We therefore conclude that the Ni dopant creates more oxygen vacancies at low P_{O_2}, which in turn increase the ionic conductivity.

The situation at high $P_{O_2}(\log P_{O_2} > -6)$ is more complicated. In general we expect the Ni^{2+} to be oxidized to Ni^{3+} as the P_{O_2} increases. For the lowest Ni concentration $(y = 0.05)$, the conductivity is seen to decrease at high P_{O_2} (Fig. 2(a)). This is consistent with the conductivity being ionic. For this low level of Ni, it is not surprising to find the width of the impurity band insufficient to support significant levels of electronic conductivity. If we have an oxidation of Ni^{2+} to Ni^{3+} then we would expect the oxygen vacancy concentration to decrease and the ionic conductivity to decrease as observed in Fig. 2(a). However, the magnitude of the decrease remains small, e.g., a factor of 1.3 between the conductivity at the plateau and the conductivity in air at 800C. Furthermore, the activation energy at high P_{O_2} is also nearly unchanged from the low P_{O_2} region suggesting that the mode of conduction has not changed. This tells us that the Ni is only slightly oxidized to Ni^{3+} and remains largely as Ni^{2+} in air. Otherwise, we would have expected a change in activation energy to accommodate the energetics associated with the oxidation of Ni. This feature will be of importance in our analysis of LSGN $(y = 0.2)$

For the remaining samples, the high P_{O_2} conductivity is either nearly P_{O_2} independent or shows a small increase with P_{O_2}. For example the conductivity of LSGN$(y = 0.2)$ has a P_{O_2} dependence of approximately $\sigma_t \approx P_{O_2}{}^{1/10}$ at 800°C. The conductivity of LSGN$(y = 0.5)$ also increases slightly in this region. These results suggest that the Ni oxidation state does not change appreciably in the $10^{-5} \leq P_{O_2} \leq 1$ atm. range as discussed above. For LSGN$(y = 0.2)$, the concentration of Ni is clearly high enough to form an impurity band which gives dominant electronic conductivity. The conductivity of LSGN$(y = 0.5)$ at 800°C of $\sigma \approx 50$ S/cm is suitable for a fuel cell electrode.

The ionic conductivities in air are extracted from analysis of the ac impedance response of the blocking cells M/LSG/LSGN/LSG/M. A typical spectrum obtained from our samples is shown in Fig. 4, along with the equivalent circuit. The high frequency intercept corresponds to the bulk resistance. At intermediate frequencies we see a depressed semicircle resulting from interfacial characteristics, i.e., the Pt/SE and/or SE/MIEC interface. At very low frequencies we see a Warburg diffusion impedance due to O^{2-} diffusion in the MIEC. A grain boundary contribution is not resolvable at the temperatures of interest here. The ac impedance spectrum shown in Fig. 4 clearly shows a low frequency feature that is not visible for a non-blocking cell, i.e., a M/LSG/M cell. To ensure that this low frequency feature was not due

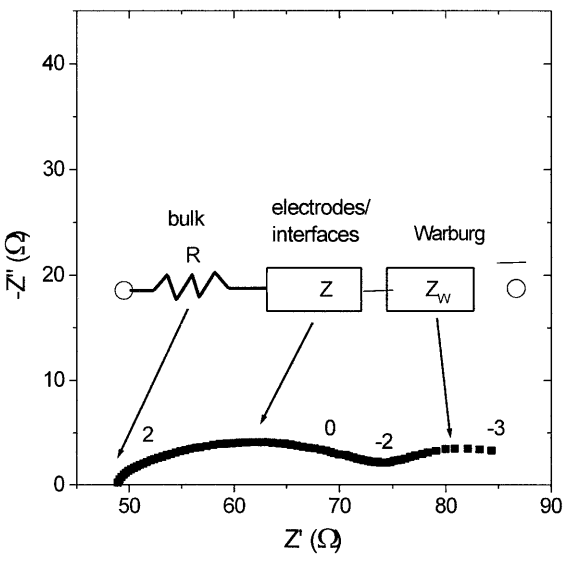

Fig. 4. AC impedance spectrum of blocking cell M/LSG/$LSGN_{10-20}$/LSG/M at 800°C in air.

to an interfacial resistance at the LSG/LSGN boundary, we constructed two blocking cells for LSGN($y = 0.2$), one with twice the length of the other. The result of fitting the Warburg feature in each case to Eq. 2 is shown in Table 2. As expected, doubling the length of the MIEC approximately doubles the resistance and changes the fitting factor S by a factor of four (as $S = L^2/12\tilde{D}$). This is evidence that the low frequency part of the spectrum is due to diffusion in the mixed conductor rather than interfacial effects.

The Warburg part of the spectrum is fitted to Eq. 1. We then use the results from the total conductivity measurement and Eqs. 2 and 3 to solve for the ionic conductivity of the LSGN. We were able to follow this procedure for the samples LSGN($y = 0.1$) and LSGN($y = 0.2$). The sample LSGN($y = 0.05$) was not considered appropriate for this technique as it is largely an ionic conductor (i.e., t_e is small so R_w will be small, note Eq. 2). We also were not able to identify a Warburg feature in the spectrum of the blocking cell with LSGN($y = 0.5$). The most likely reason for this is that the response of the metal electrodes obscured the Warburg feature. If $\tilde{D}$ increases due to an increase in the electronic and/or the ionic conductivity the features will tend to overlap. An increase in the ionic conductivity also decreases the magnitude of Z_w making it more difficult to identify.

The results of the ac blocking measurements are shown in Table 3. Both samples have ionic conductivities which are comparable to their low P_{O_2} values (see Fig. 3). Specifically, if we compare the magnitude of the conductivity of LSGN ($y = 0.2$) at the plateau at 800C ($\sigma \sim 0.16$ S/cm) with the ionic conductivity in air derived from the blocking experiment ($\sigma \sim 0.12$ S/cm; see Table 3) we find a ratio of 1.33, nearly the same ratio as obtained above for LSGN($y = 0.05$). The fact that the ionic conductivity in air doubles as the Ni content doubles clearly suggests that the Ni dopant continues to affect the ionic conductivity at high P_{O_2}. This is consistent with results on $LaCo_{1-x}Ni_xO_3$ mixed conductors in which the Ni is considered to be predominantly in the Ni^{2+} oxidation state [21].

Recently Jamnik and Maier [22] reexamined the impedance of mixed conductors with selectively blocking electrodes and derived a novel equivalent circuit with a ''chemical'' capacitor which can be related to the low frequency time constant S by

$$S \sim R_{\text{ser}} C_{\text{chem}}/12 = \frac{L^2}{12\tilde{D}} \tag{6}$$

where the series resistance is given by

$$R_{\text{ser}} = R_{\text{ion}} + R_{\text{eon}} \tag{7}$$

in which R_{ion} is the ionic and R_{eon} is the electronic component of the resistance of the MIEC. The chemical capacitance C_{chem} reflects the ability of the specimen to store chemical energy, i.e., the change in chemical potential due to stoichiometry variations. If Boltzmann statistics apply, it is given by

$$C_{\text{chem}} = \frac{q^2}{kT} AL \left(\frac{1}{z_{\text{ion}}^2 c_{\text{ion}}^2} + \frac{1}{z_{\text{eon}}^2 c_{\text{eon}}^2} \right)^{-1} \tag{8}$$

where z_{ion}, c_{ion} are the charge and concentration of ionic defects and z_{eon}, c_{eon}, are the charge and concentration of electronic defects. This expression for C_{chem} shows it to be dependent on sample volume and both ionic and electronic carrier densities. Jamnik and Maier further show that Eq. 6 holds true if one can assume that $C_{\text{chem}} \gg C_{el}$, where C_{el} is

Table 2. Fitting parameters of Warburg for different length samples

Sample	Length (mm)	$R_w(\Omega)$	S (sec)	$\tilde{D}$(cm^2/sec)	$R_{\text{ser}}(\Omega)$	$C_{\text{chem}}(F)$
LSGN($y = 0.2$) 800°C	1.57	3.2	24.7	8.34×10^{-5}	3.7	80
LSGN($y = 0.2$) 800°C	3.14	7.1	94.7	8.67×10^{-5}	7.1	160
LSGN($y = 0.1$) 925°C	1.81	1.62	24.8	1.10×10^{-4}	10.5	28

Table 3. Ionic conductivities of $LSGN_{10-y}$ compounds in air

	σ_{ionic} at 800°C	E_A (eV)
$La_{0.9}Sr_{0.1}Ga_{0.9}Ni_{0.1}O_3$	0.063	0.89
$La_{0.9}Sr_{0.1}Ga_{0.8}Ni_{0.2}O_3$	0.12	1.0

the electrode capacitance. This is the case in the present experiment given that one readily observes the Warburg impedance at low frequency [22].

With the above expressions, it becomes possible to derive the chemical diffusivity $\tilde{D}$, the chemical capacity C_{chem} and the carrier densities. First, taking the values of L and S from Table 2 and substituting them into Eq. 6, one obtains values of $\tilde{D}$ at 800°C of the order of 9×10^{-5} cm^2/s. To calculate C_{chem}, we require values for R_{ser}. First we find R_{ion} by multiplying $(\sigma_{\text{ion}})^{-1}$ from Table 3 by the geometrical factor L/A. Then from the values of R_W in Table 2 and the assistance of Eq. 2 we calculate R_{eon}. (Alternatively, combining Eqs. 2, 3 and 7 we have $R_{\text{ser}} = (R_t + R_w)^2/R_w$.) The values of R_{ser} are also listed in Table 2. Again with the aid of Eq. 6, one now calculates values for C_{chem} which come out to be tens of farads. While this sounds surprisingly high, it should be remembered that these are not electrostatic capacitors. The values for $\tilde{D}$ and C_{chem} are also listed in Table 2. One should also note that $\tilde{D}$ should not, in this case, be impacted by electron trapping effects [22] given the formation of the impurity band which enables ambipolar transport of ions as well as the electrons associated with the Ni ions.

Next we calculate the ionic mobility from the data of Fig. 3. We noted that the ionic conductivity increases linearly with the total acceptor density which corresponds to the total Sr and the divalent Ni content. Noting that the Sr content represents a concentration of 1.7×10^{21} cm^{-3}, it is straight forward to show that the ionic mobility $\mu_v = 7.35 \times 10^{-5}$ cm^2/V-s at 800°C. Taking the ionic conductivity of 0.12 S/cm from the blocking experiment for LSGN($y = 0.2$), one obtains a value for $c_{\text{ion}} = 5.1 \times 10^{21}$ cm^{-3} by using the above value for μ_v and the definition of conductivity.

It now becomes possible to calculate the concentration of electronic carriers c_{eon} with the assistance of Eq. 8 which is found to be $c_{\text{eon}} = 2.50 \times 10^{21}$ cm^{-3}. Since we view the electronic conductivity, measured at high oxygen partial pressures, as being localized in the Ni impurity band[2], it is useful to translate this value in terms of the fraction of total Ni content. This turns out to be $c_{\text{eon}} = 0.73\ [\text{Ni}_{\text{Ga}}]_{\text{total}}$ which is consistent with our expectation that electronic conduction at high P_{O_2} is via hopping in the Ni band. Under those circumstances, for significant levels of conductivity, Ni must coexist with substantial fractions in both valence states. Taking the hole density to represent roughly 3/4 of the Ni as Ni^{3+}, this leaves approximately 1/4 of the Ni as Ni^{2+}, very close to the maximum conductivity value achieved when the concentration of both valence states are equal [20][3]. One may further confirm the validity of this model by calculating the magnitude of the electronic mobility. The electronic conductivity for LSGN($y = 0.2$) in air is easily calculated from R_{eon} to be 1.6 S/cm at 800°C. Substituting this value and that for c_{eon} into the definition of conductivity, one calculates a mobility of 4.0×10^{-3} cm^2/V-s. Furthermore, one may note that the activation energy for LSGN($y = 0.2$) in air is ~ 0.14 eV. Both the magnitude and activation energy are entirely consistent with a hopping type mobility mechanism [23]. A similar analysis of the data for LSGN($y = 0.1$) leads to a value for $c_{\text{eon}} = 1.04 \times 10^{21}$ cm$^{-3} \sim 0.6[\text{Ni}_{\text{Ga}}]_{\text{total}}$. The other terms are also summarized in Table 2. Note, however, that these values for LSGN($y = 0.1$) were evaluated at a temperature of 925°C.

The magnitude of the thermal expansion of these materials is important in establishing their utility as electrodes in a monolithic cell. The thermal expansion curves for the four materials are shown in Fig. 5. There is a discontinuity in the thermal expansion at intermediate temperatures of around 750°C. Values of the thermal expansion coefficient (TEC) for the low and high temperature regions are given in Table 4. As the Ni content increases the TEC increases slightly in the low temperature region, and almost doubles in the high temperature region. The average thermal expansion of the electrolyte material $La_{0.8}Sr_{0.2}Ga_{0.85}Mg_{0.15}O_3$ is 12.4×10^{-6} K^{-1}. The highly Ni-doped materials have coefficients that differ significantly from this in the high temperature region. This may present difficulties in the preparation of electrodes made of these materials.

The reason for the high TEC at high temperature is not known at present. Preliminary high temperature XRD measurements have shown that there may be a phase change to a cubic phase at intermediate temperatures. The cubic phase may be responsible for the high thermal expansion at high temperatures.

4. Summary and Conclusions

The substitution of Ni for Ga^{3+} in the solid electrolyte $La_{0.9}Sr_{0.1}Ga_{1-y}Ni_yO_3$ results in a strong enhancement

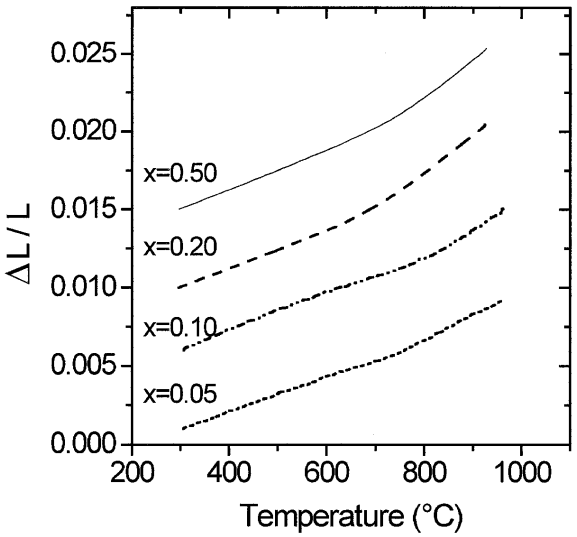

Fig. 5. Thermal expansion curves for the $La_{0.9}Sr_{0.1}Ga_{1-x}Ni_xO_3$ samples.

of the electronic conductivity at high P_{O_2}, reaching values as high as 50 S/cm in the temperature range of 600–900°C for $y = 0.5$. At low P_{O_2} the conductivity can be modeled by assuming that the Ni is in the $+2$ oxidation state and the charge is compensated by oxygen vacancies. This leads to a predominant ionic conductivity at low P_{O_2}. Evaluation of the Warburg impedance of an electronic blocking cell showed LSGN($y = 0.1$ and 0.2) to retain ionic conductivities in air comparable to the low P_{O_2} values, and comparable to other lanthanum gallate solid electrolytes. An analysis of the equivalent circuit of the Warburg impedance of LSGN($y = 0.2$) in terms of the chemical capacitance provided values, at 800°C for the chemical diffusivity $\tilde{D} \sim 9 \times 10^{-5}\,\mathrm{cm^2/s}$ and the chemical capacitance $C_{\mathrm{chem}} = 80$–$160\,\mathrm{F}$ with the latter depending on geometry. Evaluation of the dependence of ionic conductivity on dopant density provided a value for the effective oxygen vacancy mobility $\mu_v = 7.35 \times 10^{-5}\,\mathrm{cm^2/V\text{-}s}$ and carrier density $c_{\mathrm{ion}} = 1.72 \times 10^{21}\,\mathrm{cm^{-3}}$. This combined with the expression for C_{chem} enabled a determination of the electron density $c_{\mathrm{eon}} = 2.50 \times 10^{21}\,\mathrm{cm^{-3}}$ or in terms of the fraction of total Ni content, $c_{\mathrm{eon}} = 0.73[\mathrm{Ni_{Ga}}]_{\mathrm{total}}$. The calculated electronic mobility of $4.0 \times 10^{-3}\,\mathrm{cm^2/V\text{-}s}$ and activation energy of 0.14 eV for the $y = 0.2$ material are in excellent agreement with expectations of an electronic transport model involving electron hopping within the Ni impurity band. Thermal expansion measurements show good matches of the TEC with lanthanum gallate electrolytes at low and intermediate temperatures.

These results suggest that LSGN could make a good SOFC cathode compatible with a lanthanum gallate electrolyte. If the mixed conductivity is retained in the LSGN($y = 0.5$) compound, then it may have excellent catalytic properties. In a future paper we will report the results of cathodic overpotential measurements for an electrode using this material.

Acknowledgments

H.L. Tuller thanks Basic Energy Sciences, U.S. Department of Energy, for support of this research under contract #DE-FG02-86ER45261 and the Alexander von Humboldt foundation for its support during the author's visit to the Laboratory of Prof. J. Maier at The Max Planck Institute in Stuttgart, Germany in the summer of 1998. N.J. Long, thanks the NZ Foundation for Research Science and Technology for financial support. The authors thank Drs. Jamnik and Maier for their stimulating discussions regarding their impedance model for mixed conductors under selectively blocking conditions.

Notes

1. Note that a factor of $1/\pi^2$ rather than 1/12 is given by Maier in Eq. 22, ref. 12. This small difference comes from approximations used in the frequency rather than the time domain analysis [22].

Table 4. Thermal expansion coefficients of $LSGN_{x-y}$ materials

Compound	TEC (300–700°C)	TEC (800–950°C)
$La_{0.9}Sr_{0.1}Ga_{0.95}Ni_{0.05}O_3$	$11.0 \times 10^{-6}\,\mathrm{K^{-1}}$	$15.7 \times 10^{-6}\,\mathrm{K^{-1}}$
$La_{0.9}Sr_{0.1}Ga_{0.9}Ni_{0.1}O_3$	$12.4 \times 10^{-6}\,\mathrm{K^{-1}}$	$19.2 \times 10^{-6}\,\mathrm{K^{-1}}$
$La_{0.9}Sr_{0.1}Ga_{0.8}Ni_{0.2}O_3$	$12.6 \times 10^{-6}\,\mathrm{K^{-1}}$	$24.2 \times 10^{-6}\,\mathrm{K^{-1}}$
$La_{0.9}Sr_{0.1}Ga_{0.5}Ni_{0.5}O_3$	$13.2 \times 10^{-6}\,\mathrm{K^{-1}}$	$25.2 \times 10^{-6}\,\mathrm{K^{-1}}$

2. In this treatment, the Ni derived band has replaced the O2p band as the source of the valence band.
3. Note that this is not entirely consistent with our above conclusion that the Ni is largely in the $+2$ valence state. However, given the number of assumptions made to arrive at these numbers, we are satisfied with arriving at values within a factor of 2 or 3 of the correct value.

References

1. T. Ishihara, H. Matsuda, and Y. Takita, *J. Amer. Chem. Soc.*, **116**, 3801 (1994).
2. M. Feng and J.B. Goodenough, *Eur. J. Solid State Chem.*, **31**, 663 (1994).
3. K. Huang, M. Feng, J.B. Goodenough, and M. Schmerling, *J. Electrochem. Soc.*, **143**, 3630 (1996).
4. K. Huang, M. Feng, J.B. Goodenough, and C. Milliken, *J. Electrochem. Soc.*, **144**, 3620 (1997).
5. N.J. Long and H.L. Tuller, ''Mixed Ionic-Electronic Conduction in Ni-Doped Lanthanum Gallate Perovskites,'' in *Materials for Electrochemical Energy Storage and Conversion II—Batteries, Capacitors and Fuel Cells* (MRS vol. **496**) eds. D. Ginley, D. Doughty, B. Scrosati, T. Takamura, and Z. Zhang (Materials Research Society, Warrendale, PA, 1998) p. 129.
6. F. Lecarpentier, H.L. Tuller, and N.J. Long, *Performance of* $La_{0.9}Sr_{0.1}Ga_{0.5}O_3$ *as a Cathode for a Lanthanum Gallate Fuel Cell*, unpublished.
7. H.L. Tuller, S.A. Kramer, and M.A. Spears, Novel Compatible Solid Electrolyte-Electrode System Suitable for Solid State Electrochemical Cells, U.S. Patent No. 5,403,461, April 4, 1995; H.L. Tuller, in *High Temperature Electrochemistry: Ceramics and Metals*, eds., F.W. Poulsen, N. Bonanos, S. Linderoth, M. Mogensen, and B. Zachau-Christiansen, Risø National Laboratory, Røskilde, Denmark (1996), p. 139.
8. T. Ishihara, H. Furutani, H. Hishiguchi, and Y. Takita, ''Oxygen Ion Conductivity in Doped Lanthanide Gallium Based Perovskite Oxide,'' in *Ionic and Mixed Conducting Ceramics III, ECS Symposium Proceedings,* Vol. **97-24**, eds. T.A. Ramanarayanan, W.L. Worrell, and H.L. Tuller, A.C. Khandkar, M. Mogensen and W. Gopel, Paris, France (The Electrochemical Society, Pennington, NJ, 1998), p. 834.
9. P.A. Cox, in *Transition Metal Oxides: An Introduction to their Electronic Structure and Properties* (Oxford University Press, 1992), p. 233.
10. O. Porat, N. Long, and H.L. Tuller, ''Mixed Ionic-Electronic Conduction in Mn-Doped Gadolinium Titanate Pyrochlore,'' in *Ionic and Mixed Conducting Ceramics III, ECS Symposium Proceedings* Vol. 97-24, eds. T.A. Ramanarayanan, W.L. Worrell, and H.L. Tuller, A.C. Khandkar, M. Mogensen, and W. Gopel, Paris, France (The Electrochemical Society, Pennington, NJ, 1998), p. 350.
11. J.-S. Lee and H.-I. Yoo, *Solid State Ionics*, **68**, 139 (1994).
12. J. Maier, *Z. Phys. Chem. Neue Folge*, **140**, 191 (1984).
13. I. Yokota, *J. Phys. Soc. Jpn.*, **16**, 22213 (1961).
14. D.R. Franceschetti, J.R. Macdonald, and R.P. Buck, *J. Electrochem. Soc.*, **138**, 1386 (1991).
15. I. Riess, ''Critical Review of Methods for Measuring Partial Conductivities in Mixed Ionic Electronic Conductors'', in *Second Int. Symp. on Ionic and Mixed Conducting Ceramics*, T.A. Ramanarayanan, W.L. Worrell, and H.L. Tuller, Editors (The Electrochemical Society, Pennington, NJ, 1994), p. 286.
16. T. Ishihara, H. Matsuda, and Y. Takita, *Solid State Ionics*, **79**, 147 (1995).
17. T. Ishihara, J.A. Kilner, M. Honda, and Y. Takita, *J. Amer. Cer. Soc.*, **119**, 2747 (1997).
18. K. Nomura and S. Tanase, *Solid State Ionics*, **98**, 229 (1997).
19. N.J. Long, unpublished results.
20. F.A. Kroger, in *The Chemistry of Imperfect Crystals* (North Holland, Amsterdam, 1974), p. 14.
21. Y. Teraoka, T. Nobunaga, K. Okamoto, N. Miura, and N. Yamazoe, *Solid State Ionics*, **48**, 207 (1991).
22. J. Maier, *Solid State Phenomena*, **39–40**, 35–60 (1994); J. Jamnik and J. Maier, unpublished.
23. H.L. Tuller and A.S. Nowick, *J. Phys. Chem. Solids*, **38**, 859 (1977).